Thickness of ventromedial prefrontal cortex in humans is correlated with extinction memory

Mohammed R. Milad*, Brian T. Quinn†, Roger K. Pitman*, Scott P. Orr*‡, Bruce Fischl†, and Scott L. Rauch*§

*Department of Psychiatry and †Nuclear Magnetic Resonance Center, Massachusetts General Hospital and Harvard Medical School, Charlestown, MA 02129; and ‡Research Service, Veterans Affairs Medical Center, Manchester, NH 03104

Edited by Marcus E. Raichle, Washington University School of Medicine, St. Louis, MO, and approved June 3, 2005 (received for review March 24, 2005)

The ventromedial prefrontal cortex (vmPFC) has been implicated in fear extinction [Phelps, E. A., Delgado, M. R., Nearing, K. I. & Ledoux, J. E. (2004) *Neuron* 43, 897–905; Herry, C. & Garcia, R. (2003) *Behav. Brain Res.* 146, 89–96]. Here, we test the hypothesis that the cortical thickness of vmPFC regions is associated with how well healthy humans retain their extinction memory a day after having been conditioned and then extinguished. Fourteen participants underwent a 2-day fear conditioning and extinction protocol. The conditioned stimuli (CSs) were pictures of virtual lights, and the unconditioned stimulus (US) was an electric shock. On day 1, participants received 5 CS+US pairings (conditioning), followed by 10 CS trials with no US (extinction). On day 2, the CS was presented alone to test for extinction memory. Skin conductance response (SCR) was the behavioral index of conditioning and extinction. Participants underwent MRI scans to obtain structural images, from which cortical thickness was measured. We performed a vertex-based analysis across the entire cortical surface and a region-of-interest analysis of *a priori* hypothesized territories to measure cortical thickness and map correlations between this measure and SCR. We found significant, direct correlation between thickness of the vmPFC, specifically medial orbitofrontal cortex, and extinction retention. That is, thicker medial orbitofrontal cortex was associated with lower SCR to the conditioned stimulus during extinction recall (i.e., greater extinction memory). These results suggest that the size of the vmPFC might explain individual differences in the ability to modulate fear among humans.

cortical thickness | fear conditioning | orbitofrontal cortex

Extinction of conditioned fear is of substantial basic and clinical neuroscientific interest. To describe posttraumatic stress disorder (PTSD), the *Diagnostic and Statistical Manual of Mental Disorders* (1) gives the example of a woman who is raped in an elevator and subsequently comes to fear all elevators. Recovery from PTSD entails, among other things, learning not to fear situations associated with the traumatic event (i.e., to extinguish conditioned fear responses) (2). It has been reported that 2 weeks after a rape, 92% of victims met symptom criteria for PTSD, but 3 months later only 47% did (3). Such individual differences in recovery from PTSD are likely related to genetically influenced individual differences in fear extinction and its retention (4). It is quite possible that these differences are mediated by variance in regional brain structures.

Under a Pavlovian (classical) conditioning model, a once-neutral conditioned stimulus (CS) (e.g., a light) is paired with an aversive unconditioned stimulus (US) (e.g., a shock). After a few pairings, the CS comes to elicit various manifestations of a fear conditioned response, including freezing in rodents (5) and increased skin conductance in humans (6). When the CS is then repeatedly presented in the absence of the shock, the conditioned response is extinguished. There is substantial evidence indicating that fear extinction results in the formation of a new memory that coexists with, but opposes, the initial conditioning memory (7, 8). Under favorable circumstances, the extinction memory is recalled when the CS is later presented.

Convergent data from the animal literature implicate the ventral medial prefrontal cortex (vmPFC) in the recall and expression of extinction memory (5, 9). Lesion and pharmacological manipulation studies show that the vmPFC is critical for extinction recall after a delay (10, 11). Activity in single neurons recorded from the infralimbic (IL) region of the vmPFC (12), mPFC-evoked potentials (13), and vmPFC metabolism (14) are all inversely correlated with fear expression during extinction recall. Furthermore, microstimulation of IL neurons reduces conditioned freezing in rats that have been conditioned but not extinguished, simulating a postextinction state (12, 15). Thus, in rodents, the vmPFC appears to inhibit conditioned fear responses and mediate extinction recall.

Human neuroimaging studies of fear conditioning have traditionally focused on acquisition (16). However, two recent functional MRI studies investigated the neural circuitry of fear extinction. Gottfried and Dolan (17) showed increased activation in the vmPFC, including medial orbitofrontal cortex (mOFC), during extinction of aversive olfactory conditioning. Phelps *et al.* (18) found that response in vmPFC during day 2 extinction recall significantly correlated with the success of extinction training on day 1, as measured by skin conductance response (SCR), consistent with a role for the vmPFC in the retention of extinction learning. Extinction of eye-blink conditioning has also been shown to activate the mPFC (19). In addition, several imaging studies have shown that during differential conditioning, mPFC activity increases to the CS− (a stimulus that is not paired with the shock), consistent with the role of the mPFC in signaling safety (20, 21). Thus, human (v)mPFC regions appear to play a role similar to that in rodents.

Could the size of the vmPFC explain why some people have better control of their fear and, therefore, perhaps are more resilient to emotional trauma? Preliminary data from animals show that superior extinction memory performance is associated with larger IL.¶ Furthermore, morphometric studies in humans have shown reduced mPFC volume in PTSD relative to non-PTSD patients (23). The goal of the present study was to investigate whether individual differences in fear extinction relate to the size of the vmPFC in healthy humans. Therefore, we examined the relationship between brain morphometry and the results of a 2-day differential conditioning experiment during which SCRs were measured. The psychophysiological experiment we performed was originally designed to investigate the effect of context manipulations on extinction retention (24). In the present study, an automated method (25) was used to

This paper was submitted directly (Track II) to the PNAS office.

Abbreviations: vmPFC, ventromedial prefrontal cortex; CS, conditioned stimulus; US, unconditioned stimulus; SCR, skin conductance response; mOFC, medial orbitofrontal cortex; PTSD, posttraumatic stress disorder; IL, infralimbic; ROI, region of interest; rACC, rostral anterior cingulate cortex; SC, subcallosal cortex; dACC, dorsal anterior cingulate cortex; CXs, visual contexts.

§To whom correspondence should be addressed at: Department of Psychiatry, 149 13th Street, CNY 2618, Charlestown, MA 02129. E-mail: rauch@psych.mgh.harvard.edu.

¶Cintron, B. & Quirk, G. J. (2004) *Soc. Neurosci. Abstr.* **328,** 13.

www.pnas.org/cgi/doi/10.1073/pnas.0502441102

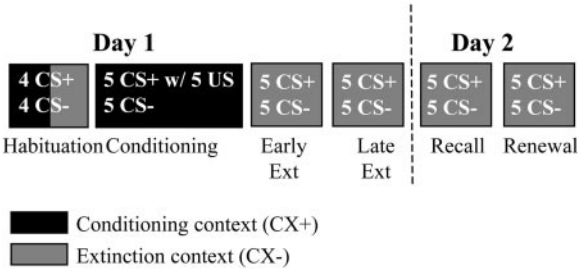

Fig. 1. Schematic of the experimental protocol. (Adapted from ref. 24). [Reproduced with permission from Milad *et al.* (24) (Copyright 2005, Blackwell Publishing).]

measure cortical thickness from the MRIs. We investigated three vmPFC *a priori* regions of interest (ROIs) (based on literature reviewed): rostral anterior cingulate cortex (rACC), subcallosal cortex (SC), and mOFC. We hypothesized that the thickness of one or more of these regions would be positively correlated with extinction retention, whereas the thickness of the dorsal anterior cingulate cortex (dACC), selected as a control region, would not. Correlations between extinction retention and thickness were first performed by using manually defined ROIs. Subsequently, a vertex-based method was used to map the topography of effects within each ROI as well as across the entire cortical surface.

Methods

Participants. Fourteen healthy volunteers (eight men and six women), 21–34 years of age and recruited from the local community by means of an advertisement, participated in this study. Written informed consent was obtained from all participants in accordance with the requirements of the Partners Health Service Human Research Committee at Massachusetts General Hospital.

Conditioning and Extinction Procedure and Psychophysiological Measures. The fear conditioning and extinction procedures used in this study were identical to those described in ref. 24. Digital photographs of two different rooms (a conference room containing books on a bookshelf and an office containing a computer on a desk) constituted the visual contexts (CXs). Each room contained a lamp, and the two different colors (blue and red) of the lighted lampshade constituted the CSs. The selection of the CS+ and CS− colors and the CX+ and CX− rooms was randomly determined and counterbalanced across participants. Contexts and CSs were displayed on a computer monitor ≈2 feet behind the participants while they were in a mock scanner. The US was a 500-ms electric shock delivered through electrodes attached to the second and third fingers of the dominant hand. The intensity of the shock was previously determined by each participant to be "highly annoying but not painful (6)."

The experimental protocol was administered over 2 days (see Fig. 1). On day 1, the habituation phase consisted of eight trials, in which the to-be CS+ and to-be CS− (four of each) were presented in a counterbalanced manner within either the to-be conditioning context (CX+) or the to-be extinction context (CX−). The conditioning phase consisted of five CS+ and five CS− trials, all presented within CX+. The US occurred immediately after each CS+ offset. The extinction phase was divided into two subphases: early and late, which were separated by an ≈1-min rest period. Each subphase consisted of five CS+ and five CS− trials, all presented within the CX−. No shocks were delivered during the extinction phase. Note that the shock electrodes remained attached to the participant's fingers during the extinction phase and all subsequent phases of the experiment. On day 2, the recall phase was identical to an extinction subphase given on day 1. During the renewal phase, five CS+ and five CS− were presented within the CX+, and again no US was delivered. In half of the participants, the renewal phase preceded the recall phase, whereas the order was reversed for the other half of the participants.

For each trial during the experiment, the context picture was presented for 18 s: 6 s alone, followed by 12 s in combination with the CS+ or CS−. The mean intertrial interval was 16 s (range, 12–21 s). A SCR score was calculated for each CS trial by subtracting the mean skin conductance level during the 2 s immediately before CS onset (during which the context alone was being presented) from the highest skin conductance level recorded during the 12-s CS duration. Thus, all SCRs to the CS+ and CS− reported herein reflect changes in the skin conductance level above and beyond any changes in skin conductance level produced by the context. Although many studies examining SCRs have used the first-interval or second-interval response, limiting our scoring of skin conductance to the first or second intervals would leave the last 4 s of the CS presentation unscored. Furthermore, it is not clear that the 12-s CS interval used in the present study can simply be divided into 6-s first- and second-response intervals. The present scoring method allows for the detection of the maximal increase in skin conductance levels at any point during the12-s presentation. We have used this method in previous, published human psychophysiological research, which has supported its validity (6, 26). Furthermore, we have previously shown that, by using the exact protocol used herein, a second-by-second analysis of change in skin conductance levels during fear conditioning for the CS+ and CS− trials shows peak responsivity occurring at ≈4–5 s after CS onset, remained high throughout the 12 s CS presentation (see Fig. 2 in ref. 24). Each skin conductance response was square-root transformed before analysis. Unless specified, all data are presented as means ± SE.

Image Acquisition and Analysis Procedures. ***Acquisition.*** A Sonata 1.5-T whole-body high-speed imaging device (Siemens, Iselin, NJ) was used with a 3-axis head coil. Structural MRI data were gathered in replicate by using a high-resolution 3D MPRAGE sequence (repetition time/time to echo/flip angle = 7.25 ms/3 ms/7°) with an in-plane resolution of 1.3 mm and a slice thickness of 1 mm.

Measurement of cortical thickness in individual participants. These methods have been described in detail in refs. 25, 28, and 29 but are briefly summarized herein. The two structural scans for each participant were averaged to create a single high signal-to-noise average volume. The resulting volume was used to segment cerebral white matter (30) and to estimate the gray/white interface. Topological defects in the gray/white estimate were fixed (31), and this gray/white estimate was used as the starting point for a deformable surface algorithm designed to find the pial surface with submillimeter precision (25). The entire cortex in each individual was then visually inspected, and any inaccuracies in segmentation were manually corrected. All of these measurement procedures were carried out by investigators who were blind to the nature of the hypotheses to be tested and blind to the corresponding SCR data.

For each participant, thickness measures across the cortex were computed by finding the point on the gray/white boundary surface that was closest to a given point on the estimated pial surface (and vice versa) and averaging between these two values (25). The accuracy of the thickness measures derived from this technique has been validated by direct comparisons with manual measures on postmortem brains (28) as well as direct comparisons with manual measures on MRI data (29).

Inflation, registration, and interparticipant averaging. The surface representing the gray/white border was "inflated" (32), differences

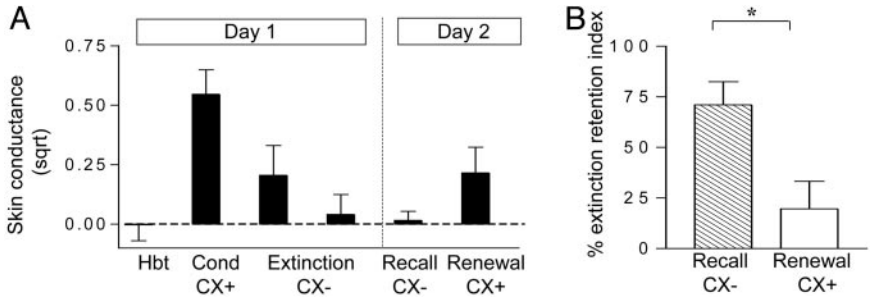

Fig. 2. Illustration of psychophysiological data. (*A*) Mean SCRs collapsed across trials for each experimental phase for the CS+. Hbt, habituation; Cond, conditioning; CX+, conditioning context; CX−, extinction context. (*B*) Extinction retention index (see text for definition) in each context. CX- corresponding to recall phase and CX+ corresponding to renewal phase. *, $P < 0.05$.

between individuals in the depth of gyri/sulci were normalized, and each participant's reconstructed brain was then morphed/registered to an average spherical surface representation that optimally aligned sulcal and gyral features across participants (32, 33). This spherical morphing procedure was used to construct the cortical thickness difference brain maps.

Computation of mean and statistical cortical thickness difference maps. The spherical transform was used to map the thickness measurements at each vertex on each participant's cortical surface into a common spherical coordinate system (32, 33). The data were smoothed on the surface tessellation by using an iterative nearest-neighbor averaging procedure (100 iterations were applied, equivalent to applying a 2D Gaussian smoothing kernel along the cortical surface with a full width half maximum of ≈13 mm).

Defining boundaries of ROIs. Boundary definition of the ROIs selected in the present study was performed as described in ref. 34. Briefly, the dACC and the rACC were divided by a coronal plane at the genu of the corpus callosum, corresponding to plane I of the methodology of Caviness *et al.* (35). More precisely, plane I contributed the anterior border of the dACC, as well as the anterior border of the SC territory. The mOFC spanned the interval between the SC and the frontal pole; the posterior boundary of the frontal pole marked the anterior border of the mOFC.

Statistical analysis. Interparticipant group averaging and inference was performed by using the spherical registration to align the surfaces, smoothing the surfaces for 100 iterations, and fitting a general linear model at each vertex of the surface. The model consisted of % extinction retention in the CX− (recall) and CX+ (renewal) contexts and cortical thickness. Each phase measurement was analyzed separately from the other because they were hypothesized to have no interaction.

Results

Psychophysiological Measures of Fear Conditioning, Extinction, Recall, and Renewal. The full results of the psychophysiology experiment are reported in ref. 24. For illustrative purposes, the mean SCRs to the five CS+ presentations for each phase in the 14 participants who also underwent MRI are presented in Fig. 2*A*.

For the purpose of morphometric correlation, the % extinction retention index was calculated as follows: each participant's SCR to the first CS+ trial during the recall and renewal phases was divided by the highest SCR to a CS+ trial during conditioning. This was then multiplied by 100 to yield a % of CR recovered. In turn, the % CR recovered was subtracted from 100% to yield an extinction retention index. Fig. 2*B* shows that 71% extinction retention was observed in the CX− during the recall phase, and 20% extinction retention was observed in the CX+ during the renewal phase, thereby supporting the context dependency of extinction retention (see ref. 24).

Correlational Analyses of ROIs. We hypothesized that the cortical thickness of our ROIs would be positively correlated with the extinction retention index. Because only a positive correlation was predicted, one-tailed tests were used. Participants underwent MRI to obtain structural images from which cortical thickness was measured. The boundaries of the ROIs were defined as described in ref. 34 and are shown in Fig. 3*A*. The average cortical thickness for each ROI was then correlated with the extinction retention index. We found that in the CX− context (recall phase), the extinction retention index was significantly correlated with the cortical thickness of mOFC ($r = 0.52$; $P =$

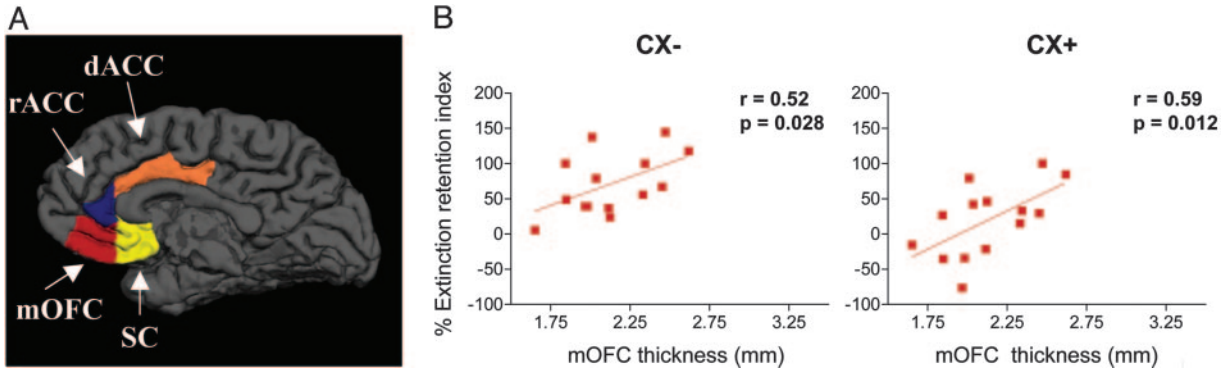

Fig. 3. Illustration of brain regions of interest and correlational plots between mOFC thickness and extinction retention. (*A*) Boundaries of ROI: SC, subcallosal cortex; mOFC, medial orbitofrontal cortex; rACC, rostral anterior cingulate cortex; dACC, dorsal anterior cingulate cortex. (*B*) Regression plots for extinction retention index separately in CX− and CX+ versus cortical thickness in mOFC.

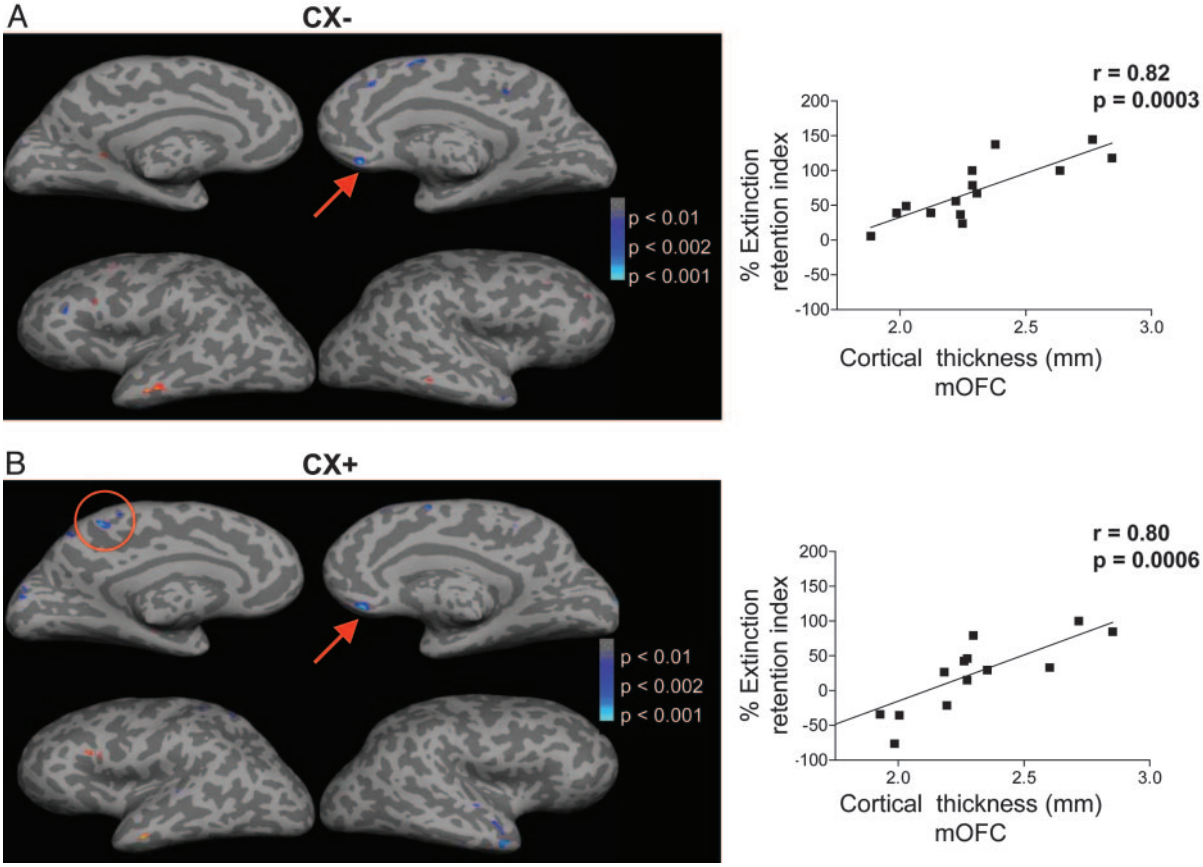

Fig. 4. Regions with positive correlations between cortical thickness and extinction retention in CX− (*A*) as well as CX+ (*B*) and regression plots for the correlations between percent extinction retention and cortical thickness in the vmPFC. Threshold is set at $P < 0.01$ (dark blue) to $P < 0.001$ (cyan blue). Red areas show incidental negative correlations. Arrow indicates vmPFC region, whereas circle indicates superior parietal correlation.

0.028) but not with SC ($r = 0.18$; $P = 0.27$), rACC ($r = 0.16$; $P = 0.29$), or dACC ($r = 0.32$; $P = 0.13$). In the CX+ context (renewal phase), the extinction retention index was again significantly correlated with the cortical thickness of mOFC ($r = 0.59$; $P = 0.012$) but not SC ($r = 0.14$; $P = 0.32$), rACC ($r = 0.10$; $P = 0.37$), or dACC ($r = 0.11$; $P = 0.34$). The regression plots for the mOFC correlations are shown in Fig. 3*B*.

Automated Vertex-Based Analyses. We also used recently developed automated methods to measure thickness across the entire cortical surface and to map correlations between this measure and extinction retention index. Vertex-based, correlational maps across the entire cortical surfaces depicting the topography of significant correlations between cortical thickness and extinction retention index at a statistical threshold of $P < 0.001$ (uncorrected, two-tailed) are shown in Fig. 4*A Left* for CX− and Fig. 4*B Left* for CX+. For the CX−, the scatterplot for the significant correlations between percent extinction retention and cortical thickness in the mOFC portion of the vmPFC [(peak vertex: $r = 0.82$, $P = 0.0003$; Talairach coordinates 4, 30, −12); ref. 22] is presented in Fig. 4*A Upper Right*. For the CX+, the scatterplot for the significant correlations between extinction retention index and cortical thickness in the mOFC portion of the vmPFC (peak vertex: $r = 0.80$, $P = 0.0006$; Talairach coordinates 6, 28, and −15) is presented in Fig. 4*B Lower Right*. Note that the average r value for the entire volume displaying significant correlation was >0.75 in both contexts. Beyond the *a priori* search territories, only one additional region in the entire brain, namely the left superior parietal cortex, exhibited a correlation with extinction retention ($P = 0.0006$) that is of comparable statistical magnitude to those observed within our *a priori* ROIs, and this was in the CX+ only (region is outlined in Fig. 4*B*). Thus, this unbiased, post hoc approach supported the specificity of our ROI findings to the vmPFC.

To rule out the possibility that the correlations we observed could be due to nonassociative processes such as sensitization, we performed correlational analyses between the mOFC cortical thickness and SCRs to the CS− during extinction recall and renewal. We found that responses to the CS− did not correlate with the cortical thickness of the mOFC ($r = 0.40$, $P = 0.15$ and $r = -0.28$, $P = 0.32$ in the CX− and CX+, respectively). In addition, to more specifically test whether the correlations described in Fig. 4 are due to associative processes, SCRs to the CS− were subtracted from those to the CS+. These differential responses were in turn correlated with the cortical thickness of the mOFC. Once more, we found significant correlations between vmPFC cortical thickness and the differential SCRs in the CX− ($r = 0.65$, $P = 0.011$) and in the CX+ ($r = 0.57$, $P = 0.035$). Thus, the correlations between the extinction retention index and mOFC cortical thickness most likely reflect associative processes mediated during and/or after extinction training. Note that no correlations were observed between mOFC cortical thickness and any other phase of the experiment [acquisition of fear conditioning or extinction training on day 1 (data not shown)].

Discussion

The results show that participants with greater vmPFC thickness, specifically thicker right mOFC, exhibited smaller SCRs to a

previously conditioned stimulus when tested a day later (i.e., they showed better extinction retention). Not only do these findings support the role of the vmPFC in the recall of extinction memory, they also provide evidence that the cortical thickness of the vmPFC, as one index of size, may explain a substantial proportion of the individual differences observed in extinction retention in humans. The implied comparable role for vmPFC in the extinction context (CX−, recall phase) as well as in the original conditioning context (CX+, renewal phase) suggests that brain regions other than vmPFC are involved in the contextual gating of extinction retention.

The correspondence between the structural vmPFC region that correlated with extinction retention in the present study, namely, the mOFC, and brain regions activated during functional extinction retention testing in humans, as well as in rodents, is striking. As noted, Phelps *et al.* (18) have recently shown that conditioned fear responses during extinction recall (as measured by skin conductance) were inversely correlated with CS+-induced activity in the vmPFC in healthy humans, indicating a direct relationship between vmPFC function and level of extinction expressed during recall. The Talairach coordinates of the vmPFC region shown to be functionally correlated with extinction recall in the study of Phelps *et al.* [4, 31, −6] are remarkably close to those shown to be structurally correlated with extinction retention in the recall and renewal phases of the present study [4, 30, −12 and 6, 28, −15, respectively]. It is important to point out that, in the present study, extinction memory was expressed best in the context in which extinction learning took place, whereas some extinction memory was still manifested in the renewal context. Thus, whereas the overall average of responses in the extinction context was lower relative to those in the conditioning context, we did observe correlations between the variance in responses to the CS+ in both contexts. Phelps *et al.* did not manipulate context during the test for extinction retention, which therefore may suggest that indeed the best comparison between our data and Phelps's study is the renewal phase. However, the coordinates for both loci of correlations were very similar. Note that these coordinates correspond to the peak vertex correlation, and that the location of the entire cluster is very comparable for both tests and also very comparable to that identified by Phelps *et al*. Other functional MRI studies have also shown activation of mOFC during extinction (17, 19, 20). As previously suggested (9), the IL region of the rat appears to be homologous to the human vmPFC. It has been shown that IL activity is inversely correlated with fear responses during extinction testing after a delay, suggesting that IL is involved in the recall of extinction memory (12). Recent preliminary data from rodents show that rats have a high behavioral variability in their recall of extinction memory 24 h after training, even when their brain function and structure are not manipulated[¶]. Interestingly, measures of IL in these animals indicated that during extinction recall, rats with larger IL cross-sectional area exhibited less freezing behavior. Thus, it appears that the size of the vmPFC may influence or predict how well fear is inhibited during extinction recall in both rodents and humans.

The thickness of the rACC, which was one of our *a priori* vmPFC brain regions, did not correlate with the recall of extinction memory. The rACC is thought to be homologous to the prelimbic (PL) region in rats (36). Phelps *et al.* (18) did not report any association between functional activity in this brain region and extinction recall in humans. Interestingly, in rats, neural activity in PL also was not correlated with extinction recall (12). Moreover, whereas IL stimulation reduced conditioned freezing, PL stimulation did not (12, 15). Barrett *et al.* (14) showed that glucose metabolism in PL did not correlate with conditioned freezing during extinction recall in mice. Thus, although the rACC is consistently implicated in emotional processing in humans, and its dysfunction is linked to various anxiety disorders (37, 38), this region does not appear to be involved in the recall of extinction memory. However, the rACC may be involved in other cognitive components of fear extinction (39). It was surprising that the thickness of the SC, another *a priori* vmPFC region, did not correlate with extinction retention. Although SC has been suggested to be a human cortical region that is homologous to that involved in fear extinction in animals, some anatomical studies suggest that the neighboring, ventral region of mPFC corresponding to the mOFC region in the present study bears an even greater homology to the IL in rats (40).

The involvement of the vmPFC in mediation of autonomic responses is well documented in rodents as well as in humans. For example, stimulation of the vmPFC in rats dampened amygdala-induced increases in blood pressure and defensive behavior (41). Human neuroimaging studies have shown that mPFC areas are functionally associated with skin conductance (42). Nagai *et al.* (43) have recently shown that activity of the vmPFC was inversely correlated with skin conductance levels during a biofeedback relaxation task. It is important to note that an association between vmPFC and skin conductance *per se* cannot account for the correlations we observed between cortical thickness and the index of extinction retention that we used, because that index is adjusted for individual differences in SC level. Specifically the extinction retention index during recall (or renewal) was calculated based on a percentage of skin conductance conditioned response during conditioning (acquisition).

The proposition that the size of a given brain region may partly explain the behavioral variance in a particular task is appealing. An increase in cortical thickness could be due to a higher number of neurons (44) or an increase in the neuropil (45). Alternatively, an increase in cortical thickness may be due to an increased number of glial cells, because recent studies have shown that cortical volume reduction observed in schizophrenic patients in the PFC is not due to the reduction of the total number of neurons but rather to the loss of glia (46). Any of these cellular differences in a brain region might better implement a function that the region subserves, e.g., in the case of the vmPFC, dampening the output of other brain regions involved in conditioned fear expression, such as the amygdala. However, it remains to be established whether in fact there is any correspondence between cortical thickness and increased (or decreased) brain function.

Several studies have suggested that larger brain regions reflect a better behavioral outcome. For example, a recent study has shown that a larger hippocampus is correlated with better recall of declarative memory (47). Conversely, studies in elderly participants show that the decrease in the capacity to recall verbal memory is associated with smaller hippocampal volumes (48). There is considerable evidence to support the association between the reduction of cortical and subcortical regions and a variety of mental disorders (49). However, larger cortical volumes have also been associated with some mental disorders. For example, increased cortical thickness in insula and rACC has been observed in patients with animal phobia (50). Larger orbitofrontal cortex has been found to be associated with decreased performance of working memory (51). Note, however, that such increases in size in pathological states may be compensatory (50).

The data presented herein suggest that the size of the vmPFC might explain individual differences in the ability to modulate fear among humans. Variability in the thickness of the vmPFC across the human population may account for risk (or resilience) factors for anxiety disorders. It is therefore of substantial interest that vmPFC appears to be functionally deficient in PTSD (reviewed in ref. 52). Specifically, neuroimaging studies have shown that when exposed to trauma-

related cues, PTSD patients show a relative failure of activation in the mPFC (37, 38, 53, 54, 55). These neuroimaging studies support the hypothesis that dysfunctional mPFC activity may underlie the exaggerated fear responses commonly observed in PTSD. It is also important to note that PTSD patients have been shown to be deficient in behavioral extinction (6). A recent morphometric study found reduced vmPFC volume in persons with PTSD compared with trauma-exposed persons without PTSD (34). Decreased PFC cortical volumes have also been observed in panic disorder (56) and obsessive–compulsive disorder (27).

Recall of extinction learning is also likely to be germane to the success of behavioral therapies, which are theoretically extinction-based. Thus, future studies should investigate whether measures of cortical thickness within the vmPFC predict therapeutic response to behavioral therapies for anxiety disorders.

We thank Dr. Gregory J. Quirk for helpful comments on the manuscript and Michelle Wedig for technical assistance. The work was supported in part by a grant from the National Institute of Mental Health (to S.L.R.) and the Massachusetts General Hospital Tosteson Fellowship (to M.R.M.). In addition, support for this research was provided in part by the National Center for Research Resources, the National Institute for Biomedical Imaging and Bioengineering, and the Mental Illness and Neuroscience Discovery Institute (to B.F.).

1. American Psychiatric Association (1994) *Diagnostic and Statistical Manual of Mental Disorders* (American Psychiatric Association, Washington, DC), 4th Ed.
2. Rothbaum, B. O. & Davis, M. (2003) *Ann. N.Y. Acad. Sci.* **1008,** 112–121.
3. Foa, E. B. (1997) *Ann. N.Y. Acad. Sci.* **821,** 410–424.
4. Fredrikson, M., Annas, P., Georgiades, A., Hursti, T. & Tersman, Z. (1993) *Biol. Psychol.* **35,** 153–163.
5. Maren, S. & Quirk, G. J. (2004) *Nat. Rev. Neurosci.* **5,** 844–852.
6. Orr, S. P., Metzger, L. J., Lasko, N. B., Macklin, M. L., Peri, T. & Pitman, R. K. (2000) *J. Abnorm. Psychol.* **109,** 290–298.
7. Quirk, G. J. (2004) *Learn. Mem.* **11,** 125–126.
8. Myers, K. M. & Davis, M. (2002) *Neuron* **36,** 567–584.
9. Milad, M. R., Rauch, S. L., Pitman, R. K. & Quirk, G. J. (2005) *Biol. Psychol.*, in press.
10. Lebron, K., Milad, M. R. & Quirk, G. J. (2004) *Learn. Mem.* **11,** 544–548.
11. Morgan, M. A., Romanski, L. M. & Ledoux, J. E. (1993) *Neurosci. Lett.* **163,** 109–113.
12. Milad, M. R. & Quirk, G. J. (2002) *Nature* **420,** 70–74.
13. Herry, C. & Garcia, R. (2002) *J. Neurosci.* **22,** 577–583.
14. Barrett, D., Shumake, J., Jones, D. & Gonzalez-Lima, F. (2003) *J. Neurosci.* **23,** 5740–5749.
15. Milad, M. R., Vidal-Gonzalez, I. & Quirk, G. J. (2004) *Behav. Neurosci.* **118,** 389–394.
16. Knight, D. C., Smith, C. N., Cheng, D. T., Stein, E. A. & Helmstetter, F. J. (2004) *Cognit. Affect. Behav. Neurosci.* **4,** 317–325.
17. Gottfried, J. A. & Dolan, R. J. (2004) *Nat. Neurosci.* **7,** 1144–1152.
18. Phelps, E. A., Delgado, M. R., Nearing, K. I. & Ledoux, J. E. (2004) *Neuron* **43,** 897–905.
19. Molchan, S. E., Sunderland, T., McIntosh, A. R., Herscovitch, P. & Schreurs, B. G. (1994) *Proc. Natl. Acad. Sci. USA* **91,** 8122–8126.
20. Morris, J. S. & Dolan, R. J. (2004) *NeuroImage* **22,** 372–380.
21. McIntosh, A. R., Rajah, M. N. & Lobaugh, N. J. (1999) *Science* **284,** 1531–1533.
22. Talairach, J. & Tournoux, P. (1988) *A Co-Planar Stereotaxic Atlas of a Human Brain* (Thieme, New York).
23. Rauch, S. L., Phillips, K. A., Segal, E., Makris, N., Shin, L. M., Whalen, P. J., Jenike, M. A., Caviness, V. S., Jr., & Kennedy, D. N. (2003) *Psychiatry Res.* **122,** 13–19.
24. Milad, M. R., Orr, S. P., Pitman, R. K. & Rauch, S. L. (2005) *Psychophysiology* **42,** 456–464.
25. Fischl, B. & Dale, A. M. (2000) *Proc. Natl. Acad. Sci. USA* **97,** 11050–11055.
26. Pitman, R. K. & Orr, S. P. (1986) *J. Abnorm. Psychol.* **95,** 208–213.
27. Szeszko, P. R., Robinson, D., Alvir, J. M., Bilder, R. M., Lencz, T., Ashtari, M., Wu, H. & Bogerts, B. (1999) *Arch. Gen. Psychiatry* **56,** 913–919.
28. Rosas, H. D., Liu, A. K., Hersch, S., Glessner, M., Ferrante, R. J., Salat, D. H., van der, K. A., Jenkins, B. G., Dale, A. M. & Fischl, B. (2002) *Neurology* **58,** 695–701.
29. Kuperberg, G. R., Broome, M. R., McGuire, P. K., David, A. S., Eddy, M., Ozawa, F., Goff, D., West, W. C., Williams, S. C., van der Kouwe, A. J., *et al.* (2003) *Arch. Gen. Psychiatry* **60,** 878–888.
30. Dale, A. M., Fischl, B. & Sereno, M. I. (1999) *NeuroImage* **9,** 179–194.
31. Fischl, B., Liu, A. & Dale, A. M. (2001) *IEEE Trans. Med. Imaging* **20,** 70–80.
32. Fischl, B., Sereno, M. I. & Dale, A. M. (1999) *NeuroImage* **9,** 195–207.
33. Fischl, B., Sereno, M. I., Tootell, R. B. & Dale, A. M. (1999) *Hum. Brain Mapp.* **8,** 272–284.
34. Rauch, S. L., Shin, L. M., Segal, E., Pitman, R. K., Carson, M. A., McMullin, K., Whalen, P. J. & Makris, N. (2003) *NeuroReport* **14,** 913–916.
35. Caviness, V. S., Jr., Kennedy, D. N., Richelme, C., Rademacher, J. & Filipek, P. A. (1996) *Cereb. Cortex* **6,** 726–736.
36. Ongur, D. & Price, J. L. (2000) *Cereb. Cortex* **10,** 206–219.
37. Bremner, J. D., Vermetten, E., Vythilingam, M., Afzal, N., Schmahl, C., Elzinga, B. & Charney, D. S. (2004) *Biol. Psychiatry* **55,** 612–620.
38. Shin, L. M., Whalen, P. J., Pitman, R. K., Bush, G., Macklin, M. L., Lasko, N. B., Orr, S. P., McInerney, S. C. & Rauch, S. L. (2001) *Biol. Psychiatry* **50,** 932–942.
39. Herry, C. & Garcia, R. (2003) *Behav. Brain Res.* **146,** 89–96.
40. Ongur, D., Ferry, A. T. & Price, J. L. (2003) *J. Comp. Neurol.* **460,** 425–449.
41. al Maskati, H. A. & Zbrozyna, A. W. (1989) *J. Auton. Nerv. Syst.* **28,** 117–125.
42. Patterson, J. C., Ungerleider, L. G. & Bandettini, P. A. (2002) *NeuroImage* **17,** 1797–1806.
43. Nagai, Y., Critchley, H. D., Featherstone, E., Trimble, M. R. & Dolan, R. J. (2004) *NeuroImage* **22,** 243–251.
44. Pakkenberg, B. & Gundersen, H. J. (1997) *J. Comp. Neurol.* **384,** 312–320.
45. Bourgeois, J. P., Goldman-Rakic, P. S. & Rakic, P. (1994) *Cereb. Cortex* **4,** 78–96.
46. Stark, A. K., Uylings, H. B., Sanz-Arigita, E. & Pakkenberg, B. (2004) *Am. J. Psychiatry* **161,** 882–888.
47. Walhovd, K. B., Fjell, A. M., Reinvang, I., Lundervold, A., Fischl, B., Quinn, B. T. & Dale, A. M. (2004) *Neurology* **63,** 1193–1197.
48. Hackert, V. H., den Heijer, T., Oudkerk, M., Koudstaal, P. J., Hofman, A. & Breteler, M. M. (2002) *NeuroImage* **17,** 1365–1372.
49. Sheline, Y. I. (2003) *Biol. Psychiatry* **54,** 338–352.
50. Rauch, S. L., Wright, C. I., Martis, B., Busa, E., McMullin, K. G., Shin, L. M., Dale, A. M. & Fischl, B. (2004) *Biol. Psychiatry* **55,** 946–952.
51. Salat, D. H., Kaye, J. A. & Janowsky, J. S. (2002) *Cereb. Cortex* **12,** 494–505.
52. Bremner, J. D. (2003) *Psychopharmacol. Bull.* **37,** 6–25.
53. Shin, L. M., Orr, S. P., Carson, M. A., Rauch, S. L., Macklin, M. L., Lasko, N. B., Peters, P. M., Metzger, L. J., Dougherty, D. D., Cannistraro, P. A., *et al.* (2004) *Arch. Gen. Psychiatry* **61,** 168–176.
54. Bremner, J. D., Staib, L. H., Kaloupek, D., Southwick, S. M., Soufer, R. & Charney, D. S. (1999) *Biol. Psychiatry* **45,** 806–816.
55. Lanius, R. A., Williamson, P. C., Boksman, K., Densmore, M., Gupta, M., Neufeld, R. W., Gati, J. S. & Menon, R. S. (2002) *Biol. Psychiatry* **52,** 305–311.
56. Vythilingam, M., Anderson, E. R., Goddard, A., Woods, S. W., Staib, L. H., Charney, D. S. & Bremner, J. D. (2000) *Psychiatry Res.* **99,** 75–82.